ISSN 3023-5669 Journal of Material Characterization and Applications, Vol. **2**, No. 1 , pp 8-16 (2024)
www.matcharappjournal.com
https://doi.org/10.5281/zenodo.11098901

PHYSICOCHEMICAL CHARACTERIZATION OF *Portulaca oleracea* L. SURFACE BY INVERSE GAS CHROMATOGRAPHY AT INFINITE DILUTION

Damla Hazal Katip[a]
Birol Işık[b]
Fatih Çakar[c]
Özlem Cankurtaran[d*]

[a] *Yildiz Technical University, Faculty of Arts & Sciences, Department of Chemistry, Esenler, Istanbul 34220, Turkey*
E-mail: hazal.katip@icloud.com

[b] *Yildiz Technical University, Faculty of Arts & Sciences, Department of Chemistry, Esenler, Istanbul 34220, Turkey*
E-mail: 19birol91@gmail.com ORCID: 0000-0002-9323-3780

[c] *Yildiz Technical University, Faculty of Arts & Sciences, Department of Chemistry, Esenler, Istanbul 34220, Turkey*
E-mail: ffatihcc@yahoo.com ORCID: 0000-0001-6192-1370

[d*] *Yildiz Technical University, Faculty of Arts & Sciences, Department of Chemistry, Esenler, Istanbul 34220, Turkey*
E-mail: kurtaran90@yahoo.com ORCID: 0000-0002-8383-1170

Received 16 February 2024; revised 20 March 2024; accepted 26 April 2024

Abstract

In this study, *Portulaca oleracea* L. plant, a low-cost biomass, was used as a stationary phase. The dispersive surface energy, acidic-basic character, enthalpy of adsorption, and Gibbs free energy of the surface of *Portulaca oleracea* L. were measured using a range of organic solvents with retention times in the infinite dilution. Using the Dorris-Gray (48.15 – 44.11 mJ/m^2), Donnet-Park (46.55 – 42.59 mJ/m^2), and Schultz (46.31 – 40.67 mJ/m^2) methods, the dispersive surface free energy was determined to decrease linearly as temperature increased. For acid-base surface interactions, the specific enthalpy of adsorption and specific adsorption-free energy were found. *Portulaca oleracea* L.'s acidic and basic characteristics were calculated with the numbers of organic solvent donors and acceptors. According to the measured values and characteristics, *Portulaca oleracea* L. has an acidic character ($K_D/K_A = 0.21$).

Keywords: Portulaca oleracea L., surface properties, inverse gas chromatography

1. Introduction

The inverse gas chromatography (IGC) technique is a highly effective, fast, easy-to-apply, and high throughput method used for the physicochemical characterization of various materials such as polymers [1], lignocellulosic materials [2], composites [3], clays [4] [5], pharmaceutical active ingredients [6], microorganisms [7], polymer blends [8], and recently various biomasses [9] [10]. The surface properties (surface energy, heat of adsorption, and acidity-basicity parameters) of such materials can be easily determined by using various solvents in volatile form and with specific properties and under conditions approaching infinite dilution of these solvents [11] [12] [13]. The IGC technique uses a solid stationary phase filled with a support material in a stainless-steel column and the column is placed in an oven. Infinitely dilute samples of solvent molecules are injected and the movement of the solvent molecules along the column and adsorption on the solid stationary phase is monitored through an inert mobile phase. As a result, net retention volumes are calculated using the retention times obtained, from which the physicochemical parameters that determine the surface properties of the solid stationary phase can be easily determined [14] [15].

One of the most important physicochemical parameters determining the surface chemistry of solid materials is the London dispersive component (γ_S^D) of the surface energy. The γ_S^D value is considered a measure of the forces of attraction between molecules due to fluctuations in the electron density of the molecules. This value can be easily determined by the IGC technique at infinitely dilute concentrations and is an extremely important parameter for characterizing the surface of the material and diversifying its uses [16] [17]. Other parameters that can be determined by the IGC technique and are very important for characterizing the surface of the material are the surface free energy of the organic molecules adsorbed on the solid surface and the acidity and basicity constants calculated based on specific interactions. The acidity-basicity constants are very important for the material surface. With the help of these parameters, it is especially important in determining which functional groups can be on the surface, the acidity-basicity behavior of the surface, and under which conditions it can be studied and provides important preliminary information in various studies, especially adsorption studies [18] [19] [20]. Although the acidity-basicity behavior of the surface can be determined by various methods such as pH_{pzc} [21], isoelectric point [22], and Boehm titration method [23], the IGC technique can give faster and more accurate results than these methods and addition to these parameters, many parameters such as dispersive surface energy and surface free energy can be easily calculated with this technique.

Natural plant-based materials and agricultural wastes have been widely used in various industrial fields, especially adsorption, due to their chemical composition, being completely natural, abundant, sustainable waste, high surface area, functionalization, antioxidant, and antimicrobial properties. To use plant-based materials in various industrial fields and to improve their properties, it is extremely important to know and determine their surface properties [24] [25] [26] [27] [28]. One such plant-based material that is abundant in nature is purslane, also known as pirpirim, whose Latin name is *Portulaca oleracea* L. This plant belongs to the family Portulacaceae and is an herbaceous annual plant that grows in warm climates. Purslane has been used as a folk remedy in many countries, acting as an antipyretic, antiseptic, and so on [29] [30].

Portulaca oleracea L. was used as a stationary phase in this work, and the surface characteristics of this plant were ascertained using the IGC technique employing infinitely dilute concentrations and solvents with distinct properties. By passing several organic solvents through the stationary phase and the inert mobile phase, retention periods were obtained. These results were used to compute the net retention volumes. This data was used to determine the surface properties of *Portulaca oleracea* L. and to build linear retention diagrams with the aid of the net retention volumes.

2. Materials and methods

Portulaca oleracea L. was purchased from herbalists in Istanbul, Turkey. All chemical materials used in the experimental studies were demonstrated in Table 1. The organic solvents given in Table 1 were used as organic solvents for the physicochemical characterization of *Portulaca oleracea* L. stationary phase and their retention behaviors were investigated by passing through the stationary phase.

Table 1. All chemical materials used in this study.

Chemicals	**Abbreviation**	**Source**	**CAS No**	**Purity (%)**
n-Hexane	Hx	Sigma Aldrich	110-54-3	≥ 99.7%
n-Heptane	Hp	Sigma Aldrich	142-82-5	≥ 99.7%
n-Octane	O	Sigma Aldrich	111-65-9	≥ 99.0%
n-Nonane	N	Sigma Aldrich	111-84-2	≥ 99.0%
n-Decan	D	Sigma-Aldrich	124-18-5	≥ 94.0%
Ethyl acetate	EA	Sigma Aldrich	141-78-6	≥ 99.8%

Acetone	Ace	Sigma Aldrich	67-64-1	≥ 99.8%
Dichloromethane	DCM	Sigma Aldrich	75-09-2	≥ 99.8%
Tetrahydrofuran	THF	Sigma Aldrich	109-99-9	≥ 99.8%
Chloroform	TCM	Sigma Aldrich	67-66-3	≥ 99.8%
Diethyl ether	DEE	Sigma Aldrich	60-29-7	≥ 99.7%

Portulaca oleracea L. plants were purchased from the herbalist and washed thoroughly with distilled water to remove external impurities. It was then dried in a vacuum oven at 105 °C for 24 h. After this process, the dry *Portulaca oleracea* L. plant was ground with the help of a grinder and passed through a sieve with a particle size range of 80-100 mesh. The powdered plant was again kept at 105 °C for 24 h to remove excess moisture from its structure and then stored in a desiccator.

Portulaca oleracea L. in dry powder form was filled into a 0.5-meter long Alltech Associates, Inc. stainless steel column in an amount of approximately 0.6 g. The ends of the stainless-steel column were plugged with a certain amount of glass wool from the same company and the surface was completely silanized. The stationary phase-filled chromatographic column was installed in Agilent Technologies 6900N gas chromatograph and conditioning was carried out at 140 °C for 24 h. During the conditioning process, the inert and high-purity Helium mobile phase was passed through the stationary phase for 24 h. Non-polar and polar organic solvents were injected into the device with a 1 μL Hamilton syringe and the solvents were allowed to drift along the column through the mobile phase and their retention behavior was investigated. To increase the accuracy of the experimental results and to ensure measurement precision, all measurements were repeated at least four times, and all results were averaged. All experimental studies were carried out at infinitely dilute concentrations. For this purpose, 0.1 μL of solvent was withdrawn with a syringe and the volume was filled to 1 μL with air and injected into the device and the retention behavior was studied.

3. Results and discussion

Physicochemical characterization of the surface of *Portulaca oleracea* L. plant was carried out in the temperature range of 30 to 55 °C. Non-polar and polar organic solvents were passed over *Portulaca oleracea* L. prepared as stationary phase and their retention behaviors were investigated and retention times were determined. Net retention volumes (V_N) were calculated by Equation (1) using the retention times of organic solvents [31] [32] [33].

$$V_N = (t_R - t_o) \times F_f \times \left(\frac{T}{T_f}\right) \times J \tag{1}$$

In this equation, t_R and t_o represent the solvent and air retention time (min), respectively; F_f represents the flow rate, T and T_f represent the chromatographic column and ambient temperature (K); J represents the James-Martin pressure compressibility correction factor [34]. With the help of the V_N values calculated using Equation (1), non-polar and polar linear retention diagrams were drawn and illustrated in Figure 1.

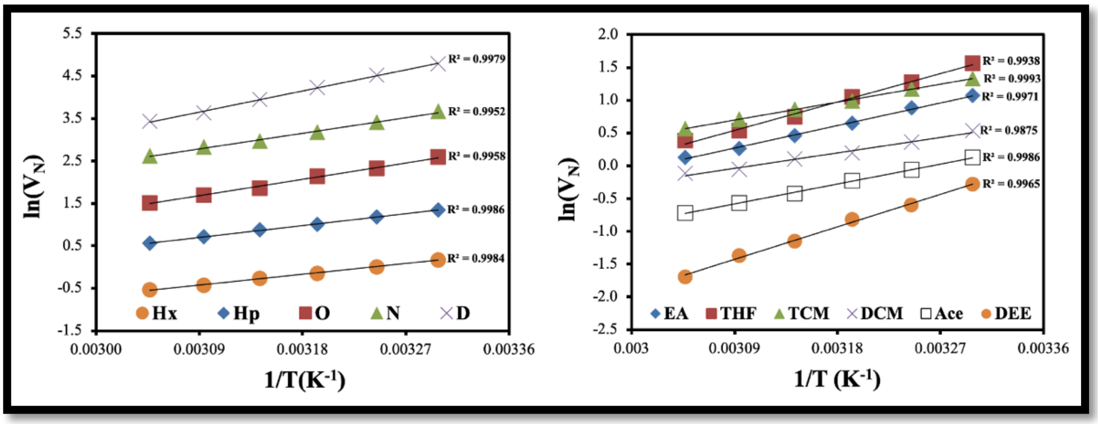

Fig. 1. The linear retention plots for non-polar and polar organic solvents on Portulaca oleracea L.

The V_N values were observed to decrease with increasing temperature, as can be seen from the linear retention diagrams in Figure 1. The V_N values in the n-alkane series were likewise found to rise as the number of carbons increased. This circumstance makes sense when considering that it was found that the adsorbent retained n-alkanes more successfully as the number of carbons increased. Depending on how polar the solvents are that are utilized, retention durations in polar solvents can change.

The adsorption of non-polar and branched hydrocarbons on the surface of a zero-density, solid mobile phase in solution occurs as a result of dispersive interactions of solvent molecules on the surface. These interactions are usually due to London-Lifshits-Van der Waals forces, also known as London dispersion forces. When non-polar organic solvent molecules adsorb at infinitely dilute concentrations, the solid adsorbs flat on the stationary phase. As a result of this adsorption process, the adsorption free energy of non-polar molecules was calculated using Equation (2) [31] [35].

$$\Delta G_{ads}(CH_2) = -R \times T \times \ln(V_N) + C \tag{2}$$

In this equation, R represents the ideal gas constant (8.314 J/mol.K), T represents the ambient temperature (K), and C represents the unidentified constant. The $\Delta G_{ads}(CH_2)$ values can be calculated from linear plots drawn between the carbon number of non-polar solvents and the $RTln(V_N)$ values. When the $\Delta G_{ads}(CH_2)$ values found in Figure 2 were investigated, it was determined that they decreased depending on the temperature.

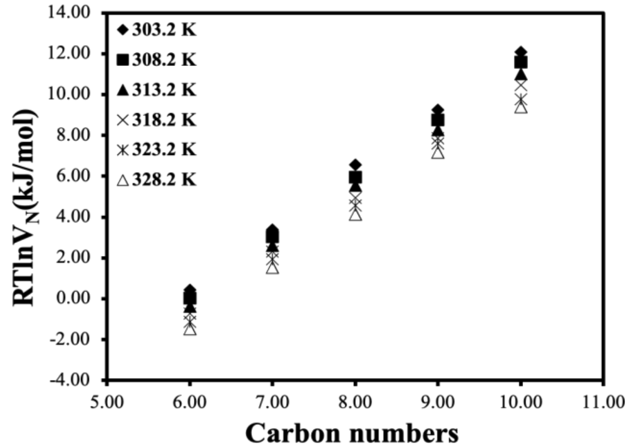

Fig. 2. The $\Delta G_{ads}(CH_2)$ values for non-polar solvents on Portulaca oleracea L. surface at different temperatures.

The dispersive component of the surface energy (γ_S^D) was calculated according to three different methods: Dorris-Gray [36], Donnet-Park [37] [38], and Schultz [39]. The γ_S^D values were calculated using Equation (3) according to the Dorris-Gray method and Equation (4) according to the Schultz method.

$$\gamma_S^D = \frac{[\Delta G_{ads}(CH_2)]^2}{4 \times N_A^2 \times \left(a_{CH_2}\right)^2 \times \gamma_{CH_2}} \tag{3}$$

$$-\Delta G_{ads} = R \times T \times \ln V_N = 2 \times N_A \times a \times (\gamma_S^D \times \gamma_L^D)^{0.5} + K \tag{4}$$

In these equations, a_{CH_2} represents the cross-section area of one methylene group (0.06 nm^2), N_A represents Avogadro's number, a represents the molecular surface area of solvents, γ_L^D represents the dispersive surface energy of solvent, γ_{CH_2} represents the dispersive surface energy of one methylene group calculated according to Dorris-Gray (Equation (5)) and Donnet-Park (Equation (6)) methods, respectively from following equations.

$$\gamma_{CH_2} = 35.6 - 0.058t \tag{5}$$

$$\gamma_{CH_2} = 35.6 - 0.058(t - 20) \tag{6}$$

The γ_S^D values of *Portulaca oleracea* L. were calculated by substituting the $\Delta G_{ads}(CH_2)$ values obtained from Figure 2, a_{CH_2} values and γ_{CH_2} values calculated from Equations (5) and (6) according to the Dorris-Gray and Donnet-Park methods, respectively, into Equation (3), and all results were listed in Table 2. According to the Schultz method, the γ_S^D values for different temperatures were calculated from the slope of the linear graphs (Figure 3 for 30 °C) drawn between $RT \ln V_N$ and $a(\gamma_L^D)^{0.5}$ using Equation (4) and listed in Table 2.

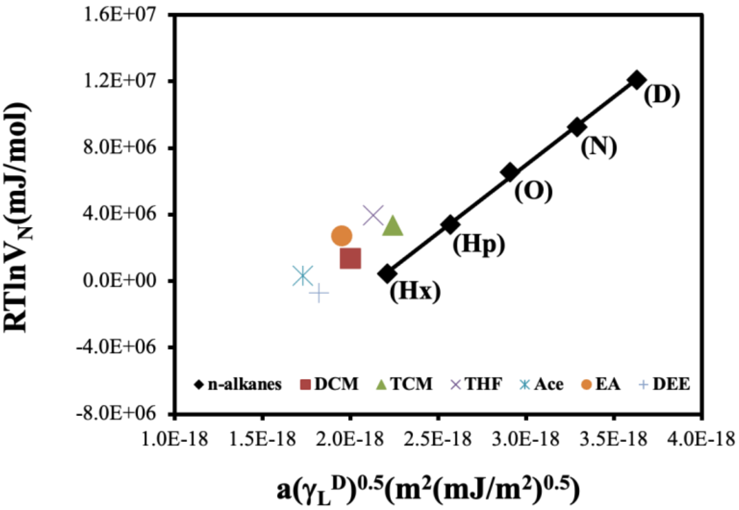

Fig. 3. The linear Schultz plot of $RT \ln(V_N)$ vs $a(\gamma_S^D)^{0.5}$ for n-alkanes and polar solvents on Portulaca oleracea L. at 30 °C.

Table 2. Dispersive surface energy (γ_S^D, mJ/m^2) values obtained from the Dorris-Gray, Donnet-Park, and Schultz methods of Portulaca oleracea L.

	Dorris-Gray			**Donnet-Park**		**Schultz**
T (°C)	**γ_{CH_2} (mJ/m^2)**	**$\Delta G_{ads}(CH_2)$ (kJ/mol)**	**γ_S^D (mJ/m^2)**	**γ_{CH_2} (mJ/m^2)**	**γ_S^D (mJ/m^2)**	**γ_S^D (mJ/m^2)**
30	33.86	-2.92	48.15	35.02	46.55	46.31
35	33.57	-2.89	47.51	34.73	45.92	45.32
40	33.28	-2.85	46.67	34.44	45.10	44.13
45	32.99	-2.79	45.08	34.15	43.55	42.29
50	32.70	-2.75	44.18	33.86	42.67	41.10
55	32.41	-2.73	44.11	33.57	42.59	40.67

Table 2 illustrates that, in the temperature range of 30 to 55 °C, the γ_S^D values obtained using the Dorris-Gray and Donnet-Park methods were higher than those obtained using the Schultz approach. This can be attributed to the way that the cross-sectional area of organic solvents varies with temperature. There are further comparable studies in the literature [40] [41] [42] [43]. Temperature dependence was discovered to be the cause of the discrepancy between the Dorris-Gray, Donnet-Park, and Schultz techniques, as the γ_S^D values drop with increasing temperatures. Stated differently, removing a substance that is attached to the surface will be considerably simpler when the temperature is high. Applying more energy will be necessary at lower temperatures. There is a difference between the two methods because the Schultz technique determines the surface area of hydrocarbon solvent molecules assuming that they are spherical, which is commonly specified as a constant. It was discovered that this disparity matched research findings from the literature [7] [44] [45].

The adsorption process of several organic solvents on the surface of *Portulaca oleracea* L. is significantly influenced by thermodynamic factors.

The properties and dynamics of adsorption processes taking place on solid surfaces can be better understood by examining these parameters. The graph presented in Figure 3 was utilized to compute the ΔG_{ads} values for polar solvents. These values, which were determined by measuring the polar solvents' separation from the hydrocarbon linear line in Figure 3, are summarized in Table 3. As seen in Table 3, polar solvents typically adsorb spontaneously on *Portulaca oleracea* L. surfaces. Taking into account their magnitudes, it was also observed that ΔG_{ads} values dropped with rising temperatures. Thus, it can be said that in this case, the adsorption of polar solvents onto the surface of *Portulaca oleracea* L. occurs more spontaneously at low temperatures.

Table 3. The variation of $-\Delta G_{ads}$ (kJ/mol), between Portulaca oleracea L. and the polar solvents for the studied temperatures.

T (°C)	**EA**	**Ace**	**DCM**	**TCM**	**THF**	**DEE**
30	4.32	3.74	2.56	2.60	4.09	1.96
35	4.27	3.64	2.54	2.66	3.82	1.52
40	4.05	3.53	2.47	2.63	3.53	1.26
45	3.86	3.20	2.53	2.65	3.20	0.60
50	3.66	3.13	2.44	2.63	3.00	0.27
55	3.31	2.70	2.26	2.27	2.62	-0.67

From the ΔG_{ads} values, the adsorption enthalpy (ΔH_{ads}) and entropy (ΔS_{ads}) values for polar solvents were determined from the following equation [46] [47]:

$$-\frac{\Delta G_{ads}}{T} = -\frac{\Delta H_{ads}}{T} + \Delta S_{ads} \qquad (7)$$

The ΔH_{ads} values were determined from Equation (7) and the results were given in Table 4. From Table 4, it was found that there is an order between ΔH_{ads} values as follows: DEE > THF > EA > Ace > DCM > TCM. ΔH_{ads} values were found to be negative for polar solvents. This situation illustrates that the adsorption process of polar solvents has an exothermic nature. From this order, DEE interacts more with basic surfaces because it is an acidic solvent, while TCM interacts less because it is a basic solvent.

Table 4. $-\Delta H_{ads}$ (kJ/mol) values of Portulaca oleracea L. for the polar solvents.

Polar Solvents	**Ace**	**EA**	**THF**	**DCM**	**TCM**	**DEE**
ΔH_{ads} **(kJ/mol)**	15.91	16.50	21.83	5.51	5.47	32.27

Determination of the acidity-basicity behavior of the surface of *Portulaca oleracea* L. is extremely important for the prediction of the functional groups that may be present on the surface and to have an idea about which types of organic pollutants can be removed from wastewater in adsorption studies [48] [49] [50] [51]. The acidity or basicity behavior can be investigated from the following equation according to the approach proposed by Gutmann [52].

$$-\Delta H_{ads} = K_A \times (DN) + K_D \times (AN^*) \qquad (8)$$

In this equation, K_A and K_D are the Lewis acid and base constant, respectively, DN and AN^* are the Gutmann's donor number and acceptor number, respectively. From Equation (8), a linear plot was drawn between DN/AN^* and $-\Delta H_{ads}/AN^*$ values using the $-\Delta H_{ads}$ values in Table 3 and was given in Figure 4. From the slope and intersection point of the linear plot in Figure 3, K_A and K_D values were determined as 0.2549 and 0.0536, respectively. The K_D/K_A value obtained by dividing these two values was calculated as 0.21. In this case, since $K_D/K_A = 0.21 < 1$, it can be said that the *Portulaca oleracea* L. surface has acidic character.

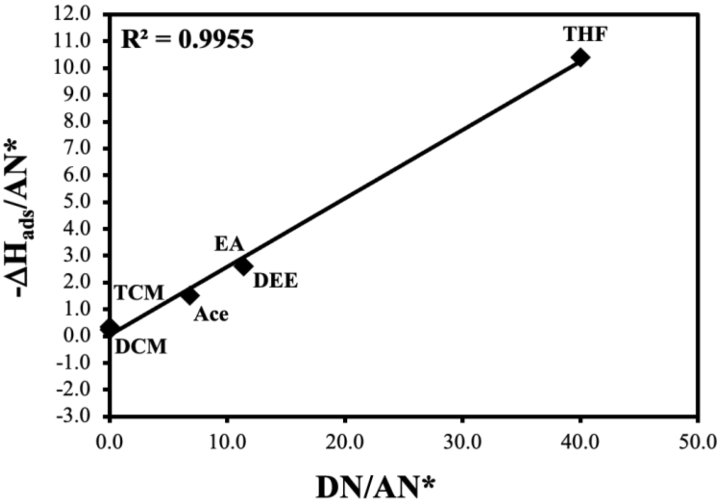

Fig. 4. The plot of $-\Delta H_{ads}/AN^*$ vs DN/AN^* of Portulaca oleracea L.

4. Conclusions

In this study, the *Portulaca oleracea* L. plant was used as a stationary phase and its surface properties were characterized by the IGC method at infinitely dilute concentrations. The retention behavior of organic solvents over the *Portulaca oleracea* L. stationary phase was investigated and linear retention diagrams were drawn. From these diagrams, the γ_S^D values of *Portulaca oleracea* L. were calculated according to four different methods: Dorris-Gray, Donnet-Park, and Schultz. It was found that the γ_S^D values ranged between 48.15 – 44.11 mJ/m^2 according to the Dorris-Gray method, 46.55 – 42.59 mJ/m^2 according to the Donnet-Park method, and 46.31 – 40.67 mJ/m^2 according to the Schultz method. The γ_S^D values calculated according to different methods were found to be high and decreased linearly with increasing temperature. The K_D/K_A value of 0.21 indicated that the surface of *Portulaca oleracea* L. has an acidic structure. Negative ΔH_{ads} and ΔG_{ads} values showed that the adsorption of polar organic solvents on *Portulaca oleracea* L. was exothermic and spontaneous.

References

[1] C. Panayiotou, Thermodynamic characterization of polymers, Polymer **136**, 47-61 (2018).
[2] J. A. F. Gamelas, The surface properties of cellulose and lignocellulosic materials assessed by inverse gas chromatography: a review, Cellulose **20**(6), 2675-2693 (2013).
[3] B. Szczepanik, D. Banas, A. Kubala-Kukus, K. Szary, P. Slomkiewicz, N. Redzia and L. Frydel, Surface properties of halloysite-carbon nanocomposites and their application for adsorption of paracetamol, Materials **13**(24), 5647 (2020).
[4] S. Bensalem, B. Hamdi, S. Del Confetto and R. Calvet, Characterization of surface properties of chitosan/bentonite composites beads by inverse gas chromatography, International Journal of Biological Macromolecules **166**, 1448-1459 (2021).
[5] S. Bensalem, B. Hamdi, S. Del Confetto, M. Iguer-Ouada, A. Chamayou, H. Balard and R. Calvet, Characterization of chitosan/montmorillonite bionanocomposites by inverse gas chromatography, Colloids and Surfaces A: Physicochemical and Engineering Aspects **516**, 336-344 (2017).
[6] I. M. Grimsey, J. C. Feeley and P. York, Analysis of the surface energy of pharmaceutical powders by inverse gas chromatography, Journal of Pharmaceutical Sciences **91**(2), 571-583 (2002).
[7] B. Isik and M. Bilgi, Investigation of physicochemical characteristics of *Aspergillus niger* biomass and examination of its ability to separate butyl acetate isomers, Applied Biochemistry Biotechnology, 1-19 (2024).
[8] F. Cakar, O. Yazici, D. Sakar, O. Cankurtaran and F. Karaman, Surface analysis of poly(ether imide) by inverse gas chromatography, Optoelectronics and Advanced Materials-Rapid Communications **5**(8), 821-826 (2011).
[9] B. Isik, Adsorptive removal of Congo red and methylene blue dyes from aqueous solutions by *Rumex obtusifolius* roots, Korean Journal of Chemical Engineering **40**(12), 3003-3016 (2023).

[10] B. Isik, F. Cakar and O. Cankurtaran, A comparative study of surface properties of *Urtica dioica* (nettle) leaves, roots, and seeds and examination of their ability to separate xylene isomers, Phytochemical Analysis **33**(6), 886-894 (2022).

[11] T. Hamieh, Study of the temperature effect on the surface area of model organic molecules, the dispersive surface energy and the surface properties of solids by inverse gas chromatography, Journal of Chromatography A **1627**, 461372 (2020).

[12] S. Mohammadi-Jam and K. E. Waters, Inverse gas chromatography applications: A review, Advances in Colloid and Interface Science **212**, 21-44 (2014).

[13] T. Hamieh, A. Abbasian and N. Farshchi, New methods to characterize the surface and interface acid–base properties of some hydrocarbons by inverse gas chromatography, Chromatographia **83**(5), 615-629 (2020).

[14] N. Cordeiro, M. Ornelas, A. Ashori, S. Sheshmani and H. Norouzi, Investigation on the surface properties of chemically modified natural fibers using inverse gas chromatography, Carbohydrate Polymers **87**(4), 2367-2375 (2012).

[15] N. Cordeiro, C. Gouveia and M. J. John, Investigation of surface properties of physico-chemically modified natural fibres using inverse gas chromatography, Industrial Crops and Products **33**(1), 108-115 (2011).

[16] T. Hamieh, Inverse gas chromatography to characterize the surface properties of solid materials, Chemistry of Materials **36**(5), 2231-2244 (2024).

[17] A. Voelkel, B. Strzemiecka, A. A. Marek and J. Zawadiak, Inverse gas chromatography investigation of oxidized polyolefins: Surface properties, Journal of Chromatography A **1337**, 194-201 (2014).

[18] B. Isik, S. Avci, F. Cakar and O. Cankurtaran, Adsorptive removal of hazardous dye (crystal violet) using bay leaves (*Laurus nobilis* L.): surface characterization, batch adsorption studies, and statistical analysis **30**, 1333-1356 (2023).

[19] V. Ugraskan, B. Isik, O. Yazici and F. Cakar, Removal of Safranine T by a highly efficient adsorbent (*Cotinus Coggygria* leaves): Isotherms, kinetics, thermodynamics, and surface properties, Surfaces and Interfaces **28**, 101615 (2022).

[20] E. Tekneci Akgul, B. Isik, B. Filiz Senkal and O. Cankurtaran, Trisurethane functionalized sulfonamide based polymeric sorbent: Synthesis, surface properties and efficient mercury sorption from wastewater, Separation and Purification Technology **325**, 124606 (2023).

[21] K. Litefti, M. S. Freire, M. Stitou and J. Gonzalez-Alvarez, Adsorption of an anionic dye (Congo red) from aqueous solutions by pine bark, Scientific Reports **9**(1), 16530 (2019).

[22] N. M. Mahmoodi, M. Arami, H. Bahrami and S. Khorramfar, Novel biosorbent (Canola hull): Surface characterization and dye removal ability at different cationic dye concentrations, Desalination **264**(1-2), 134-142 (2010).

[23] D. L. Postai, C. A. Demarchi, F. Zanatta, D. C. C. Melo and C. A. Rodrigues, Adsorption of rhodamine B and methylene blue dyes using waste of seeds of *Aleurites Moluccana*, a low cost adsorbent, Alexandria Engineering Journal **55**(2), 1713-1723 (2016).

[24] T. Uddin, A. Rahman, Rukanuzzaman and A. Islam, A potential low cost adsorbent for the removal of cationic dyes from aqueous solutions, Applied Water Science **7**(6), 2831-2842 (2017).

[25] G. Mosoarca, C. Vancea, S. Popa, M. Dan and S. Boran, The use of bilberry leaves (*Vaccinium myrtillus* L.) as an efficient adsorbent for cationic dye removal from aqueous solutions, Polymers **14**(5), 978 (2022).

[26] F. Amalina, A. Syukor Abd Razak, S. Krishnan, H. Sulaiman, A. W. Zularisam and M. Nasrullah, Advanced techniques in the production of biochar from lignocellulosic biomass and environmental applications, Cleaner Materials **6**, 100137 (2022).

[27] L. Bulgariu, L. B. Escudero, O. S. Bello, M. Iqbal, J. Nisar, K. A. Adegoke, F. Alakhras, M. Kornaros and I. Anastopoulos, The utilization of leaf-based adsorbents for dyes removal: A review, Journal of Molecular Liquids **276**, 728-747 (2019).

[28] S. Yadav, A. Yadav, N. Bagotia, A. K. Sharma and S. Kumar, Adsorptive potential of modified plant-based adsorbents for sequestration of dyes and heavy metals from wastewater - A review, Journal of Water Process Engineering **42**, 102148 (2021).

[29] C. Nurfaizah, D. Krisdiyanto, K. Khamidinal and S. Sudarlin, Krokot extract (*Portulaca Oleracea*. L) as natural light-harvesting pigments for dye-sensitized solar cells (DSSCs) : Influence of dye acidity, Biology, Medicine & Natural Product Chemistry **4**(1), 17 (2015).

[30] G. D. Saratale, R. G. Saratale, S. K. Cho, G. Ghodake, R. N. Bharagava, Y. Park, S. I. Mulla, D. S. Kim, A. Kadam, S. Nair and H. S. Shin, Investigation of photocatalytic degradation of reactive textile dyes by Portulaca oleracea-functionalized silver nanocomposites and exploration of their antibacterial and antidiabetic potentials, Journal of Alloys and Compounds **833**, 155083 (2020).

[31] B. B. Hole, D. S. Keller, W. M. Burry and J. A. Schwarz, Surface energetics of bone mineral and synthetic hydroxyapatite using inverse gas chromatography, Journal of Chromatography B **879**(21), 1847-1850 (2011).

[32] A. B. Nastasovic, N. L. Ignjatovic, D. P. Uskokovic, D. D. Markovic, B. M. Ekmescic, D. D. Maksin and A. E. Onjia, Determination of thermodynamic interactions of poly(l-lactide) and biphasic calcium phosphate/poly(l-lactide) composite by inverse gas chromatography at infinite dilution, Journal of Materials Science **49**(14), 5076-5086 (2014).

[33] B. Isik, F. Cakar, O. Cankurtaran and H. Cankurtaran, Liquid crystal entrapped porous films for ammonia sensing and determination of surface properties of liquid crystal molecule, ChemistrySelect **6**(26), 6740-6747 (2021).

[34] A. T. James and A. J. P. Martin, Gas-liquid partition chromatography: the separation and micro-estimation of volatile fatty acids from formic acid to dodecanoic acid, Biochemical Journal **50**(5), 679-690 (1952).

[35] A. C. Adiguzel, B. Korkmaz, F. Cakar, O. Cankurtaran and B. F. Senkal, Investigation of the surface properties of dibutyl amine modified poly(styrene) based polymer by inverse gas chromatography method, Journal of Polymer Research **28**(3), 83 (2021).

[36] G. M. Dorris and D. G. Gray, Adsorption of n-alkanes at zero surface coverage on cellulose paper and wood fibers, Journal of Colloid and Interface Science **77**(2), 353-362 (1980).

[37] J. B. Donnet and S. J. Park, Surface characteristics of pitch-based carbon fibers by inverse gas chromatography method, Carbon **29**(7), 955-961 (1991).

[38] J. B. Donnet, S. J. Park and H. Balard, Evaluation of specific interactions of solid surfaces by inverse gas chromatography, Chromatographia **31**(9-10), 434-440 (1991).

[39] J. Schultz, L. Lavielle and C. Martin, The role of the interface in carbon fibre-epoxy composites, The Journal of Adhesion **23**(1), 45-60 (1987).

[40] I. Erol, F. Cakar, H. Ocak, H. Cankurtaran, O. Cankurtaran, B. Bilgin-Eran and F. Karaman, Thermodynamic and surface characterisation of 4-[4-((S)-citronellyloxy)benzoyloxy]benzoic acid thermotropic liquid crystal, Liquid Crystals **43**(1), 142-151 (2016).

[41] A. Askin and D. Topaloglu Yazici, Surface characterization of sepiolite by inverse gas chromatography, Chromatographia **61**(11-12), 625-631 (2005).

[42] D. P. Kamdem, S. K. Bose and P. Luner, Inverse gas chromatography characterization of birch wood meal, Langmuir **9**(11), 3039-3044 (1993).

[43] V. Ugraskan, B. Isik, O. Yazici and F. Cakar, Surface characterization and synthesis of boron carbide and silicon carbide, Solid State Sciences **118**, 106636 (2021).

[44] W. Wang, Q. Wang, J. Tang, Q. Wang and B. Wang, Characterization of the thermodynamic properties of ionic liquid 1-allyl-3-vinylimidazolium bis((trifluorompropyl)sulfonyl)imide by inverse gas chromatography, The Journal of Chemical Thermodynamics **150**, 106236 (2020).

[45] S. Mutlu Yanic, F. Cakar, H. Ocak, F. Karaman, O. Cankurtaran and B. Bilgin Eran, Thermodynamic characterization of surface and solubility of 5-((*S*)-3,7-dimethyloctyloxy)-2-[[[4-(octyloxy)phenyl]imino]methyl]phenol liquid crystal with some solvents, Journal of Chemical & Engineering Data **64**(3), 1007-1013 (2019).

[46] A. van Asten, N. van Veedendal and S. Koster, Surface characterization of industrial fibers with inverse gas chromatography, Journal of Chromatography A **888**(1-2), 175-196 (2000).

[47] J. Kolodziejek, E. Glowka, K. Hyla, A. Voelkel, J. Lulek and K. Milczewska, Relationship between surface properties determined by inverse gas chromatography and ibuprofen release from hybrid materials based on fumed silica, International Journal of Pharmaceutics **441**(1-2), 441-448 (2013).

[48] M. N. Belgacem, G. Czeremuszkin, S. Sapieha and A. Gandini, Surface characterization of cellulose fibres by XPS and inverse gas chromatography, Cellulose **2**(3), 145-157 (1995).

[49] A. C. Adiguzel, B. Korkmaz, F. Cakar, B. F. Senkal and O. Cankurtaran, Application of inverse gas chromatography in the surface characterization of diethanol amine modified polystyrene based polymer, Turkish Journal of Chemistry **45**(5), 1533-1542 (2021).

[50] J. A. F. Gamelas and A. G. Martins, Surface properties of carbonated and non-carbonated hydroxyapatites obtained after bone calcination at different temperatures, Colloids and Surfaces A: Physicochemical and Engineering Aspects **478**, 62-70 (2015).

[51] M. Faria, F. Mohammadkazemi, R. Aguiar and N. Cordeiro, Agro-industrial byproducts as modification enhancers of the bacterial cellulose biofilm surface properties: An inverse chromatography approach, Industrial Crops and Products **177**, 114447 (2022).

[52] V. Gutmann, The donor-acceptor approach to molecular interactions, New York: Plenum (1978).